Critical exponent analysis of lightly germanium-doped $La_{0.7}Ca_{0.3}Mn_{1-x}Ge_xO_3$ (x = 0.05 and x = 0.07)

Dwi Nanto, Budhy Kurniawan, Bambang Soegijono, Nilotpal Ghosh, Jong-Soon Hwang, and Seong-Cho Yu

Citation: AIP Advances **8**, 047204 (2018);
View online: https://doi.org/10.1063/1.4993412
View Table of Contents: http://aip.scitation.org/toc/adv/8/4
Published by the American Institute of Physics

Critical exponent analysis of lightly germanium-doped $La_{0.7}Ca_{0.3}Mn_{1-x}Ge_xO_3$ (x = 0.05 and x = 0.07)

Dwi Nanto,[1] Budhy Kurniawan,[2,b] Bambang Soegijono,[2] Nilotpal Ghosh,[3] Jong-Soon Hwang,[4] and Seong-Cho Yu[4,a]

[1]*Dept. of Physics Education, Syarif Hidayatullah State Islamic University, Jakarta 15412, Indonesia*
[2]*Dept. of Physics, University of Indonesia, Depok 16424, Indonesia*
[3]*School of Advanced Sciences, VIT University, Vellore 632014, Tamilnadu, India*
[4]*Physics Department, Chungbuk National University, Cheongju 361-763, South Korea*

(Received 28 June 2017; accepted 21 September 2017; published online 19 October 2017)

We have used a critical behavior study of $La_{0.7}Ca_{0.3}MnO_3$ (LCMO) manganite perovskites whose Mn sites have been doped with Ge to explore magnetic interactions. Light Ge doping of 5 or 7 percent tended to produce LCMOs with second order magnetic transitions. The critical parameters of 5- and 7-percent Ge-doped LCMO were determined to be $T_C = 185$ K, $\beta = 0.331 \pm 0.019$, and $\gamma = 1.15 \pm 0.017$; and $T_C = 153$ K, $\beta = 0.496 \pm 0.011$, and $\gamma = 1.03 \pm 0.046$, respectively, via the modified Arrott plot method. Isothermal magnetization data collected near the Curie temperature (T_C) was split into a universal function with two branches $M(H,\varepsilon) = |\varepsilon|^{\beta} f_{\pm}(H/|\varepsilon|^{\beta+\gamma})$, where $\varepsilon=(T-T_C)/T_C$ is the reduced temperature. f_+ is used when $T>T_C$, while f_- is used when $T<T_C$. Such results demonstrate the existence of ferromagnetic short-range order in lightly Ge-doped LCMOs. Notably, doping with Ge at high concentrations tends to generate long-range ferromagnetic order.
https://doi.org/10.1063/1.4993412

I. INTRODUCTION

Modern society has developed refrigeration and uses it daily. Refrigeration has become a significant part of the food distribution system, and the food industry employs both chilling and freezing to slow the physical, microbiological, and chemical activities that cause food deterioration. Food is cooled from ambient temperature to above 0 °C when chilled and to between −18 °C (255 K) and −35 °C (238 K) when frozen.[1] Unfortunately, conventional mechanical refrigeration technologies contribute significantly to the environmental impacts of the food sector via both direct and indirect greenhouse gas emissions. To reduce these environmental emission impacts, worldwide research and development efforts have been aimed at improving refrigeration performance and developing new refrigeration technologies with the potential for reduced environmental impact.[1] Magnetic refrigeration is among the cooling technologies with a high level of current research activity. Unfortunately, implementation is not imminent, as better magnetocaloric materials and other fundamental breakthroughs are needed to achieve alternative cooling and near-room-temperature refrigeration technologies.[2]

Recently, Tagliafico *et al.* reported a linear reciprocating magnetic refrigerator prototype that achieves a maximum temperature difference of 5.0 K. Their technology operates near room temperature, under free-run conditions. Their active material includes gadolinium plates, and their process is based on the active magnetic regenerative thermodynamics cycle.[3] However, the commercial price

[a]Corresponding Email: scyu@cbnu.ac.kr
[b]bkuru@fisika.ui.ac.id

of pure gadolinium metal is $450 per 100 g. Therefore, alternative materials based on manganite perovskites have been proposed. In contrast to gadolinium, pure manganese costs $6.5 per 100 g. One can find a brief overview of the magnetocaloric effects associated with manganite perovskites in a study by Phan *et al.*[4]

The Curie temperature, T_C, is important to the characterization of magnetic cooling materials. It is the point at which a ferromagnetic material becomes paramagnetic. Thus, the phase transition from a paramagnetic (PM) insulator to ferromagnetic (FM) should be analyzed via a critical exponent study designed around the Curie temperature. Ahmed *et al.* reported that the T_C values of materials in the $La_{0.7}Ca_{0.3}Mn_{1-x}Ge_xO_3$ (x = 0.02, 0.03, 0.04, 0.06 and 0.08) series first decrease and then increase with x. The Curie temperatures recorded were -74.2 °C, -85.2 °C, -40.1 °C, -50.8 °C, and -108.7 °C, respectively.[5] This T_C fluctuation is recurrent behavior of magnetisation and resistivity due to formation of Ge pairs next to Mn^{+3}/Mn^{+4} pairs that can be explained by Zener bond blocking via single site Ge-substitution in $La_{0.7}Ca_{0.3}MnO$.[6] In addition, Ge doping provides an extreme example of carrier trapping due to formation of magnetic or lattice polarons. In the former case, carriers are confined in a finite region, though not necessarily an isolated lattice site, and the trapping centers can be thermally active.[7–10] A systematic difference between Mn^{3+} and Mn^{4+} substitution might be expected in B-site doping, which reduces the mobile electron content directly, e.g., when Mn^{4+} or Mn^{3+} (hole) is replaced. This mechanism tends to distort the local lattice by forming a Jahn–Teller polaron, while a hole does not. The concentrations of the two carriers can vary in manganese oxides.[7] In this work, we report a critical behavior analysis of polycrystalline $La_{0.7}Ca_{0.3}Mn_{1-x}Ge_xO_3$ (x = 0.05 and x = 0.07). The critical parameters of 5- and 7-percent Ge-doped LCMO were determined to be T_C = 185 K, β = 0.331 ± 0.019, and γ = 1.15 ± 0.017; and T_C = 153 K, β = 0.496 ± 0.011, and γ = 1.03 ± 0.046, respectively, via the modified Arrott plot method. Our work may contribute further to the work by Ahmed *et al.*, in which the T_C values of lightly Ge-doped $La_{0.7}Ca_{0.3}Mn_{1-x}Ge_xO_3$ vary non-linearly.[5]

II. EXPERIMENTAL

Polycrystalline $La_{0.7}Ca_{0.3}Mn_{1-x}Ge_xO_3$, ($x$ = 0.05 and 0.07) was synthesized from high-purity La_2O_3, $CaCO_3$ $MnCO_3$, and GeO_2 via a conventional solid-state reaction technique which the same technique was used by ref. 5. The sample was prepared at 1000 °C for 12 h, and then ground, pressed, and finally sintered at 1200 °C for 24 h. X-ray diffraction (XRD) patterns of all samples were measured using a Brucker AXS D8 Discover system with Cu K–α radiation at room temperature. The magnetic properties of the compound were characterized by using a vibrating sample magnetometer (VSM).

III. RESULTS AND DISCUSSION

The crystal structure of $La_{0.7}Ca_{0.3}Mn_{1-x}Ge_xO_3$ (x = 0.05 and x = 0.07) was investigated via X-ray diffraction. The lattice parameters obtained are a = 5.46 Å, b = 7.73 Å, c = 5.48 Å, and volume = 231 Å^3; and a = 5.45 Å, b = 7.69 Å, c = 5.47 Å, and volume = 229 Å^3 for x = 0.5 and x = 0.07, respectively. The XRD patterns indicate clean, single-phase orthorhombic polycrystalline structures with space group *Pbnm*, as depicted in Fig. 1. The lattice parameters of the Ge-doped samples do not differ substantially.

We also collected magnetothermal data to determine whether the magnetization versus temperature curve exhibits a gradual FM to PM transition or drops sharply. A continuous FM to PM transition is associated with a second-order magnetic phase transition (SOMT), while a sharp drop is associated with a first-order magnetic phase transition (FOMT). In the present work, both LCMO samples exhibit gradual FM to PM transitions as the temperature increases under an external field of 100 Oe (figure not shown). We also investigated isothermal magnetization of both samples around the phase transition temperature (T_C). Using the isothermal data, we obtained the slope of the H/M versus M^2 curve. The Banerjee criterion can confirm that the sample exhibits a SOMT if the slope is positive or a FOMT if the slope is negative.[11] Both samples have positive slopes and thus exhibit SOMTs, as shown in Fig. 2.

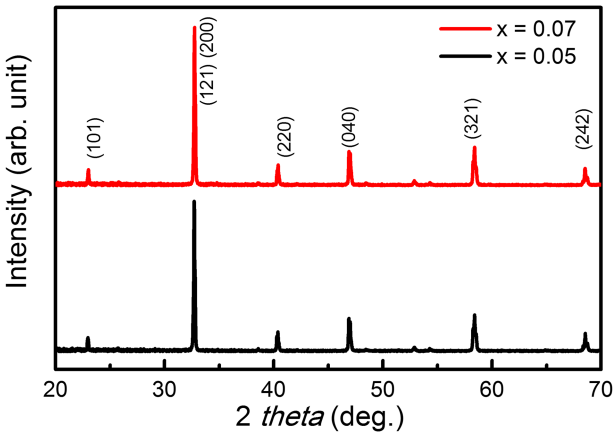

FIG. 1. XRD patterns of $La_{0.7}Ca_{0.3}Mn_{1-x}Ge_xO_3$ (x = 0.05 and 0.07).

According to the Arrott technique, a plot of H/M versus M^2 should exhibit parallel linear curves in high fields near T_C. This is based on mean-field theory and critical exponent values of $\beta = 0.5$ and $\gamma = 1$. Mean-field theory is intertwined with long-range FM order. If the plot of H/M versus M^2 is not nonlinear-parallelized, then mean-field theory cannot be used to describe magnetism in the present samples. Therefore, it is important to determine the exponential parameters β and γ of the samples.

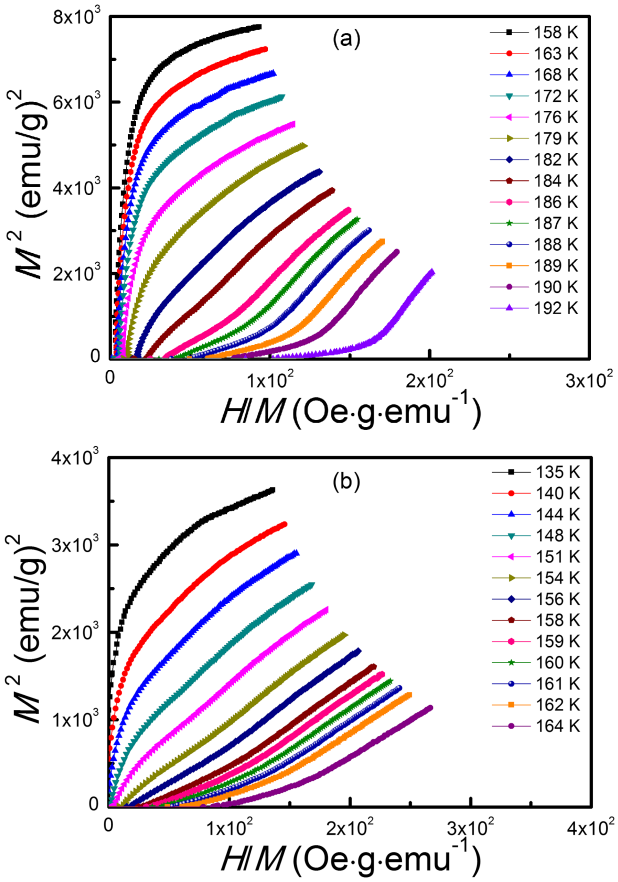

FIG. 2. Isothermal magnetization of M^2 versus H/M for $La_{0.7}Ca_{0.3}Mn_{1-x}Ge_xO_3$: (a) x = 0.05 and (b) x = 0.07.

The critical exponents β and γ obtained via fitting are associated with spontaneous magnetization and initial magnetic susceptibility, which can be used to describe a system of magnetic interactions theoretically. The β and γ values can be determined using a modified Arrott method by plotting $(H/M)^{1/\gamma}$ versus $M^{1/\beta}$, where trivial critical exponents of β=0.5 and γ=1 (from the mean-field theory model) are used as starting points. Then, one might measure spontaneous magnetization versus temperature in the high-magnetic field region based upon the intersection of the straight extrapolation line with the axis. Similarly, the relationship between initial magnetic susceptibility and temperature is determined inversely from the intersection with the axis. Near the T_C, $M_S(T)$ and χ_0^{-1} (T) are described by the following power law dependence relations:[12]

$$M_S(T) = M_0(-\varepsilon)^{\beta}, \qquad \varepsilon < 0 \tag{1}$$

$$\chi_{0^{-1}}(T) = (h_0/M_0)\,\varepsilon^{\gamma}, \qquad \varepsilon > 0 \tag{2}$$

$$M = DH^{1/\delta}, \qquad \varepsilon = 0 \tag{3}$$

where M_0, h_0, and D are the critical amplitudes, and $\varepsilon = (T - T_C)/T_C$ is the reduced temperature. According to Eq. (1) the slope obtained from the straight-line extrapolation fitting of log $[M_S(T)]$ versus log (ε) produces a new value for β. Similarly, Eq. (2) indicates that the straight-line extrapolation fitting of log $[(\chi_0^{-1}(T)]$ versus log (ε) produces a new γ. Thus, the free parameter T_C in Eq. (1) and (2) is adjusted to yield the best fit while also fitting the straight-line extrapolation system.

The Arrott plot is nonlinear and exhibits upward curvature even in the high-field regime, indicating that a case where β = 0.5 and γ = 1 does not satisfy the Arrott-Noakes equation of state

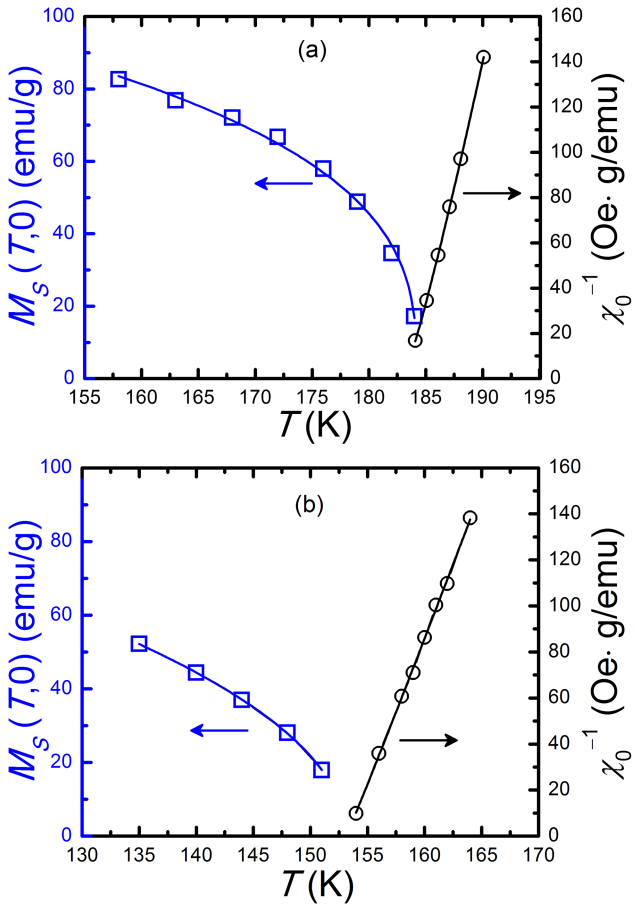

FIG. 3. Fitting curves based on the critical law. $M_S(T)$ (left axis-open square) and $\chi_0^{-1}(T)$ (right-axis open circle) for $La_{0.7}Ca_{0.3}Mn_{1-x}Ge_xO_3$: (a) x = 0.05 and (b) x = 0.07.

$(H/M)^{(1/\gamma)} = (T-T_C)/T_C + (M/M_1)^{1/\beta}$.[13] Thus, the Landau phase transition and the mean field theories based upon $\beta = 0.5$ and $\gamma = 1$ are not valid for the $La_{0.7}Ca_{0.3}Mn_{0.095}Ge_{0.05}O_3$ and $La_{0.7}Ca_{0.3}Mn_{0.093}Ge_{0.07}O_3$ systems. Therefore, modified Arrott plots were used to obtain the proper β and γ values from the following equation of state:

$$(H/M)^{(1/\gamma)} = a(T - T_C)/T_C + bM^{1/\beta}, \tag{4}$$

where a and b are constants. If β and γ are selected properly, the transform of the isothermal curve becomes a set of close, parallel straight lines in the high-field region. To determine the correct β and γ, we tested trial values of β and γ and evaluated their applicability to the mean-field theory model. These values of β and γ were substituted into Eq. (4) to generate graphs similar to those in Fig. 4 (not shown). In the high-field region, we perform linear extrapolation of the isothermal data to give $(M_S)^{1/\beta}$ and $(\chi_0^{-1})^{1/\gamma}$ as intercepts on the $(M)^{1/\beta}$ and $(H/M)^{1/\gamma}$ axes, respectively. The new values of β and γ are repeatedly used to reconstruct new modified Arrott plots until stable values of, β, γ, and T_C are obtained. After this routine, a set of reasonably good straight, parallel lines are generated alongside several parameters: $\beta = 0.331 \pm 0.019\,315$ and $\gamma = 1.15 \pm 0.017$ for $x = 0.05$; $\beta = 0.496 \pm 0.011$ and $\gamma = 1.03 \pm 0.046$ for $x = 0.07$. Fig. 3 shows the final β and γ values based on $M_S(T)$ and $\chi_0^{-1}(T)$ as functions of temperature. We shall use average values ($T_C = 185$ K for $x = 0.05$ and $T_C = = 153$ K for $x = 0.07$) for the following calculations and discussion.

The magnetic equation of state can be expressed using the variables $M(H,\varepsilon)$, H, and T. The former variable can be defined via the scaling hypothesis:

$$M(H, \varepsilon) = |\varepsilon|^{\beta} f_{\pm}(H/|\varepsilon|^{\beta+\gamma}), \tag{5}$$

where f_+ for $T > T_C$ and f_- for $T < T_C$ are regular analytic functions. After renormalization of Eq. (5), it appears that for the correct scaling relations and proper choice of β and γ values, the scaled

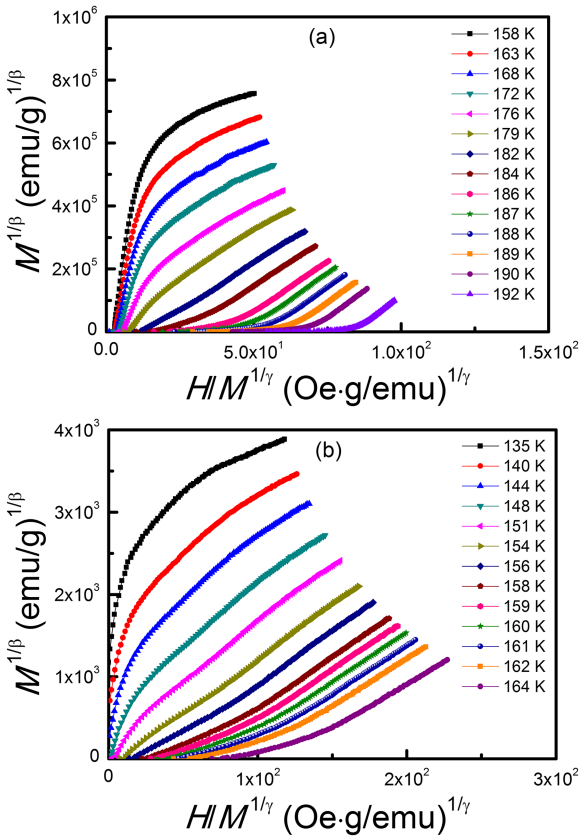

FIG. 4. Modified Arrot plots of $M^{1/\beta}$ versus $(H/M)^{1/\gamma}$ for $La_{0.7}Ca_{0.3}Mn_{1-x}Ge_xO_3$, based on the best values of β and γ: (a) $x = 0.05$ and (b) $x = 0.07$.

function falls on two universal group curves, with some curves above T_C and other curves below T_C. The Landau theory of phase transition expresses the Gibbs free energy G as a function of the order parameter M:

$$G(T, M) = G_0 + aM^2 + bM^4 - MH. \tag{6}$$

where coefficients a and b are temperature-dependent.[14] Upon applying an equilibrium condition ($dG/dM = 0$, i.e., energy minimum), the magnetic equation of state becomes:

$$H/M = 2a + 4bM^2 \tag{7}$$

Therefore, H/M versus M^2 appears linear in the high-field region of the Arrott plot. Eq. 7 is yielded from derivate of Eq. 6 then Eq. 7 can be used to produce modified Arrott plots at various temperatures. The intercept of H/M versus M^2 on the H/M axis is positive/negative above/below the T_C. The H/M versus M^2 lines that indicate T_C should cross the origin as plotted in Fig. 4.

The resulting β and γ values can be examined via scaling theory. Eq. 5 implies that $M|\varepsilon|^{\beta}$ versus $H/|\varepsilon|^{(\beta+\gamma)}$ should produce two universal curves: one set for temperatures below T_C, and another for those above T_C. Scaled data for the $x = 0.05$ and $x = 0.07$ samples is shown in Figs. 5a and 5b, respectively, based on the final values of β and γ determined above. One can observe that all of the high-field data points fall on two individual branches of $T_C > T$ and $T < T_C$. This means that the $La_{0.7}Ca_{0.3}Mn_{1-x}Ge_xO_3$ samples undergo SOMT. However, scaling describes most high fields, although it is poor in low-magnetic fields because of the rearrangement of magnetic domains and the effect of uncertainty in calculating the demagnetization factor, which can influence this region significantly. The separate branches indicate clearly that the interaction is suitably renormalized in the critical region using the scaling equation of state.

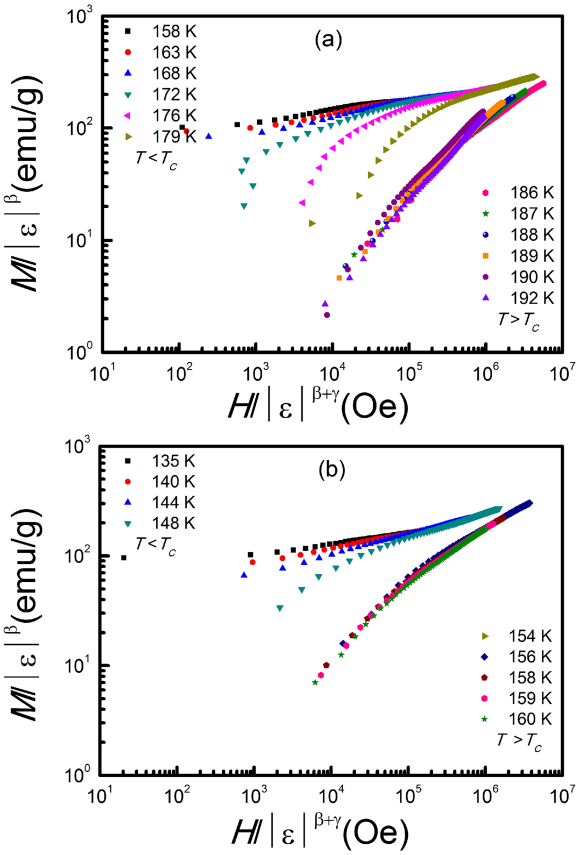

FIG. 5. Scaling plots of $La_{0.7}Ca_{0.3}Mn_{1-x}Ge_xO_3$, where (a) $x = 0.05$ and (b) $x = 0.07$. The plots indicate two universal curves below and above T_C.

These results prove that FM interactions in $La_{0.7}Ca_{0.3}Mn_{1-x}Ge_xO_3$ ($x = 0.05$ and $x = 0.07$) have the following properties: (i) they follow a short-range interaction model in which the estimated exponents are between the values expected for the 3D Heisenberg and 3D Ising models (ii) they are long-range interactions because the calculated exponents are near those associated with the mean-field model. The final β values of the $x = 0.05$ sample are between those expected for the 3D Heisenberg and 3D Ising models, and become close to those required for the mean-field model upon increased Ge doping, as shown by the $x = 0.07$ sample. It is thought that lightly Ge-doped samples in which Ge^{4+} ions replace the Mn^{4+} ions are not robust enough to influence the colossal magnetic ordering from ferromagnetic to paramagnetic, as would be indicated by a first-order magnetic phase transition of $La_{0.7}Ca_{0.3}MnO_3$. Increasing the Ge doping concentration weakens the Jahn-Teller effect and suppresses short-range magnetic interactions. According to Millis polaron theory,[15] the Jahn-Teller effect is assumed from the electron-phonon coupling and lattice distortions that split the on-site orbital degeneracy of the levels/symmetry distortions of the oxygen octahedra around a Mn site. Increasing the substitution of Mn^{4+} with Ge^{4+} might decrease the Mn^{3+}/Mn^{4+} ratio and electron-phonon coupling strength.

IV. CONCLUSIONS

We successfully synthesized $La_{0.7}Ca_{0.3}Mn_{1-x}Ge_xO_3$ ($x = 0.05$ and $x = 0.07$) via solid-state reactions and studied their magnetic interactions via critical exponent analysis. Doping of Ge onto the Mn sites in $La_{0.7}Ca_{0.3}MnO_3$ might be evidence of direct substitution of Mn^{4+} that causes magnetic ordering to transform from short-range to long-range, as described by the β and γ values obtained. Thus, Ge doping might also weaken electron-phonon coupling.

ACKNOWLEDGMENTS

This work was primarily supported by Chungbuk National University, South Korea. DN received partial support for this work from Syarif Hidayatullah State Islamic University via an international collaborative research grant (Un.01/KPA/568/2017). BK was partially supported by a grant from the Ministry of Research, Technology and Higher Education, the Republic of Indonesia Government via Universitas Indonesia (contract for PUPT grant no. 2699/UN.2.R3.1/HKP.05.00/2017).

[1] S. A. Tassou, J. S. Lewis, Y. T. Ge, A. Hadawey, and I. Chaer, "A review of emerging technologies for food refrigeration applications," Applied Thermal Engineering **30**, 263–276 (2010).
[2] J. Steven Brown and P. A. Domanski, "Review of alternative cooling technologies," Applied Thermal Engineering **64**, 252–262 (2014).
[3] L. A. Tagliafico, F. Scarpa, F. Valsuani, and G. Tagliafico, "Preliminary experimental results from a linear reciprocating magnetic refrigerator prototype," Applied Thermal Engineering **52**, 492–497 (2013).
[4] M.-H. Phan and S.-C. Yu, "Review of the magnetocaloric effect in manganite materials," J. Magn. Magn. Mater. **308**, 325–340 (2007).
[5] A. M. Ahmed, V. Morchshakov, K. Bärner, C. P. Yang, P. Terzieff, H. Schicketanz, T. Gron, J. R. Sun, and G. H. Rao, "Recurrent behavior of magnetisation and resistivity in Ge-substituted $La_{0.7}Ca_{0.3}MnO_3$," Phys. Stat. Sol. (A) **200**, 407–414 (2003).
[6] A. M. Ahmed, A. Kattwinkel, N. Hamad, K. Bärner, J. R. Sun, G. H. Rao, H. Schicketanz, P. Terzieff, and I. V. Medvedeva, "Evidence for magnetic clustering around Ge-sites in fixed valence doped manganites $La_{0.7}Ca_{0.3}Mn_{1-y}Ge_yO_3$," J. Magn. Magn. Mater. **242-245**(Part 2), 719–721 (2002).
[7] J. R. Sun, G. H. Rao, B. G. Shen, and H. K. Wong, "Doping effects arising from Fe and Ge for Mn in $La_{0.7}Ca_{0.3}MnO_3$," Appl. Phys. Lett. **73**, 2998–3000 (1998).
[8] W. Archibald, J. S. Zhou, and J. B. Goodenough, "First-order transition at T_C in the orthomanganites," Phys. Rev. B **53**, 14445–14449 (1996).
[9] J. S. Zhou, W. Archibald, and J. B. Goodenough, "Identification of a new type of electronic state in the magnetoresistive orthomanganites," Nature **381**, 770–772 (1996).
[10] J. M. D. Coey, M. Viret, L. Ranno, and K. Ounadjela, "Electron localization in mixed-valence manganites," Phys. Rev. Lett. **75**, 3910–3913 (1995).
[11] B. K. Banerjee, "On a generalised approach to first and second order magnetic transitions," Phys. Lett. **12**, 16–17 (1964).
[12] H. E. Stanley, *Introduction to Phase Transitions and Critical Phenomena* (Oxford University Press, London, U.K., 1971).
[13] A. Arrott and J. E. Noakes, "Approximate equation of state for nickel near its critical temperature," Phys. Rev. Lett. **19**, 786–789 (1967).
[14] P. L. Ivy, *Magnetism and Superconductivity* (Springer, Berlin, 2002).
[15] A. J. Millis, R. Mueller, and B. I. Shraiman, "Fermi-liquid-to-polaron crossover. II. Double exchange and the physics of colossal magnetoresistance," Phys. Rev. B **54**, 5405–5417 (1996).